



This is a repository copy of *Combining crystallization-driven self-assembly with reverse sequence polymerization-induced self-assembly enables the efficient synthesis of hydrolytically degradable anisotropic block copolymer nano-objects directly in concentrated aqueous media.*

White Rose Research Online URL for this paper:

<https://eprints.whiterose.ac.uk/214281/>

Version: Published Version

Article:

Farmer, M.A.H. orcid.org/0009-0008-9645-6921, Musa, O.M. and Armes, S.P. orcid.org/0000-0002-8289-6351 (2024) Combining crystallization-driven self-assembly with reverse sequence polymerization-induced self-assembly enables the efficient synthesis of hydrolytically degradable anisotropic block copolymer nano-objects directly in concentrated aqueous media. *Journal of the American Chemical Society*, 146 (24). pp. 16926-16934. ISSN 0002-7863

<https://doi.org/10.1021/jacs.4c06299>

Reuse

This article is distributed under the terms of the Creative Commons Attribution (CC BY) licence. This licence allows you to distribute, remix, tweak, and build upon the work, even commercially, as long as you credit the authors for the original work. More information and the full terms of the licence here:

<https://creativecommons.org/licenses/>

Takedown

If you consider content in White Rose Research Online to be in breach of UK law, please notify us by emailing eprints@whiterose.ac.uk including the URL of the record and the reason for the withdrawal request.



eprints@whiterose.ac.uk
<https://eprints.whiterose.ac.uk/>

Combining Crystallization-Driven Self-Assembly with Reverse Sequence Polymerization-Induced Self-Assembly Enables the Efficient Synthesis of Hydrolytically Degradable Anisotropic Block Copolymer Nano-objects Directly in Concentrated Aqueous Media

Matthew A. H. Farmer, Osama M. Musa, and Steven P. Armes*



Cite This: *J. Am. Chem. Soc.* 2024, 146, 16926–16934



Read Online

ACCESS |



Metrics & More

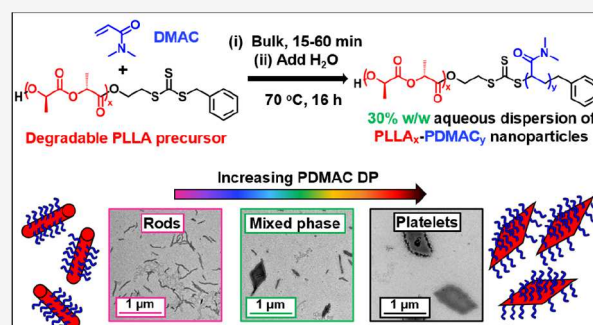


Article Recommendations



Supporting Information

ABSTRACT: Herein we combine the well-known processing advantages conferred by polymerization-induced self-assembly (PISA) with crystallization-driven self-assembly (CDSA) to achieve the efficient synthesis of hydrolytically degradable, highly anisotropic block copolymer nano-objects directly in aqueous solution at 30% w/w solids. This new strategy involves a so-called reverse sequence PISA protocol that employs poly(L-lactide) (PLLA) as the crystallizable core-forming block and poly(*N,N'*-dimethylacrylamide) (PDMAC) as the water-soluble non-ionic coronal block. Such syntheses result in PDMAC-rich anisotropic nanoparticles. Depending on the target diblock copolymer composition, either rod-like nanoparticles or diamond-like platelets can be obtained. Furthermore, *N*-Acryloylmorpholine is briefly evaluated as an alternative hydrophilic vinyl monomer to DMAC. Given that the PLLA block can undergo either hydrolytic or enzymatic degradation, such nanoparticles are expected to offer potential applications in various fields, including next-generation sustainable Pickering emulsifiers.



INTRODUCTION

Following pioneering studies by Manners and Winnik, crystallization-driven self-assembly (CDSA) is now well-established as a synthetic route to highly anisotropic block copolymer rods and other interesting morphologies such as diamond-like platelets.^{1–11} CDSA typically utilizes an insoluble crystalline block and a soluble steric stabilizer block. Most studies are conducted at high dilution in a range of organic solvents, but CDSA can also be achieved in (dilute) aqueous solution, which is preferred for potential bioapplications.^{7,12–15}

Unlike CDSA, polymerization-induced self-assembly (PISA) normally involves growing an insoluble amorphous block from a soluble precursor block.^{16–21} Depending on the target diblock copolymer composition, this approach typically yields spheres, worms, or vesicles.²² Recently, we reported a counterintuitive reverse sequence aqueous PISA formulation in which a hydrophobic precursor is solubilized in concentrated aqueous media using a water-miscible vinyl monomer as a cosolvent.²³ Polymerization of this monomer gradually worsens the solvency for the growing amphiphilic diblock copolymer chains, which subsequently undergo *in situ* self-assembly to form spheres. Herein, we combine the processing advantages offered by reverse sequence PISA with CDSA to prepare highly anisotropic hydrolytically degradable block copolymer nano-objects directly in aqueous media at 30% w/w

solids.²⁴ This new strategy involves a hydroxy-functional trithiocarbonate reagent,^{7,10,25,26} employs poly(L-lactide) (PLLA) as the crystallizable core-forming block, and uses poly(*N,N'*-dimethylacrylamide) (PDMAC) as the water-soluble non-ionic coronal block (see Scheme 1).

RESULTS AND DISCUSSION

Recently, we reported a reverse sequence PISA formulation based on a hydrophobic poly(ϵ -caprolactone) (PCL) precursor, which exhibits a melting transition, T_m , at approximately 50 °C. In this prior study, the *in situ* DMAC polymerization was performed at 80 °C, which results in the formation of spherical PCL–PDMAC nanoparticles with amorphous cores.²³ In contrast, PLLA has a T_m of 114–153 °C (see Figure S1). Hence reverse sequence PISA syntheses performed at 70 °C should lead to the formation of anisotropic PLLA–PDMAC nanoparticles with semicrystalline cores via CDSA (see Scheme 1).

Received: May 8, 2024

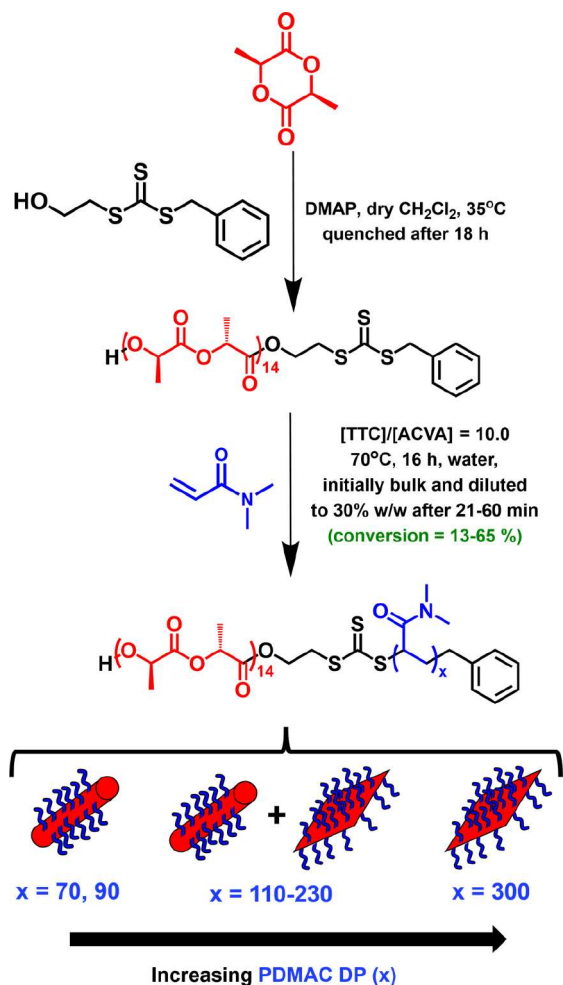
Revised: May 16, 2024

Accepted: May 17, 2024

Published: June 6, 2024



Scheme 1. Synthesis of a 30% w/w Aqueous Dispersion of PLLA₁₄-PDMAC_x Diblock Copolymer Nanoparticles by the Judicious Combination of Reverse Sequence PISA with CDSA^a



^aA PLLA₁₄-TTC precursor is first prepared via anionic ring-opening polymerization of L-lactide at 35 °C using a hydroxy-functional RAFT agent as an initiator. The RAFT polymerization of DMAC is then conducted in the bulk at 70 °C. At a suitable intermediate DMAC conversion, the reaction mixture is diluted with deionized water to induce self-assembly of the growing amphiphilic PLLA₁₄-PDMAC_x diblock copolymer chains.

In the present study, the anionic ring-opening polymerization of L-lactide was initiated using a hydroxy-functional reversible addition-fragmentation chain transfer (RAFT) agent in the presence of a 4-(dimethylamino)pyridine (DMAP) catalyst, as previously reported.²⁵ Anhydrous conditions ensured controlled polymerization to produce a hydrophobic semicrystalline poly(L-lactide) PLLA precursor with a mean degree of polymerization (DP) of 14 as determined by end-group analysis using ¹H NMR spectroscopy. More specifically, the integrated oxymethine PLLA signal at 5.21 ppm was compared to the integrated aromatic proton signals assigned to the benzyl end-group at 7.29–7.41 ppm (see Figures S2 and S3). Furthermore, UV GPC analysis (λ = 305 nm) confirmed the absence of any unreacted RAFT agent after purification of PLLA₁₄-TTC (see Figure S4).

This PLLA₁₄-TTC precursor was then dissolved in *N,N*-dimethylacrylamide (DMAC) and RAFT polymerization of

this vinyl monomer was conducted in the bulk^{27,28} at 70 °C. Once a significant increase in solution viscosity was observed (corresponding to a DMAC conversion of 13–65%), degassed deionized water (preheated to 70 °C) was added to the reaction mixture to target a final solids content of 30% w/w (see Scheme 1). The DMAC polymerization was allowed to proceed for 16 h at 70 °C before quenching by cooling the reaction mixture to 20 °C with concomitant exposure to air. For the synthesis of a PLLA₁₄-PDMAC₁₂₀ diblock copolymer, the reaction mixture was periodically sampled, and aliquots were analyzed by GPC and ¹H NMR spectroscopy to study the polymerization kinetics. After 100 min at 70 °C, 99% DMAC conversion was achieved (Figure 1a).

Remarkably, there was no discernible reduction in the rate of polymerization after dilution of the initial bulk reaction mixture to 30% w/w solids. This is presumably because acrylamides polymerize much faster in aqueous media than in

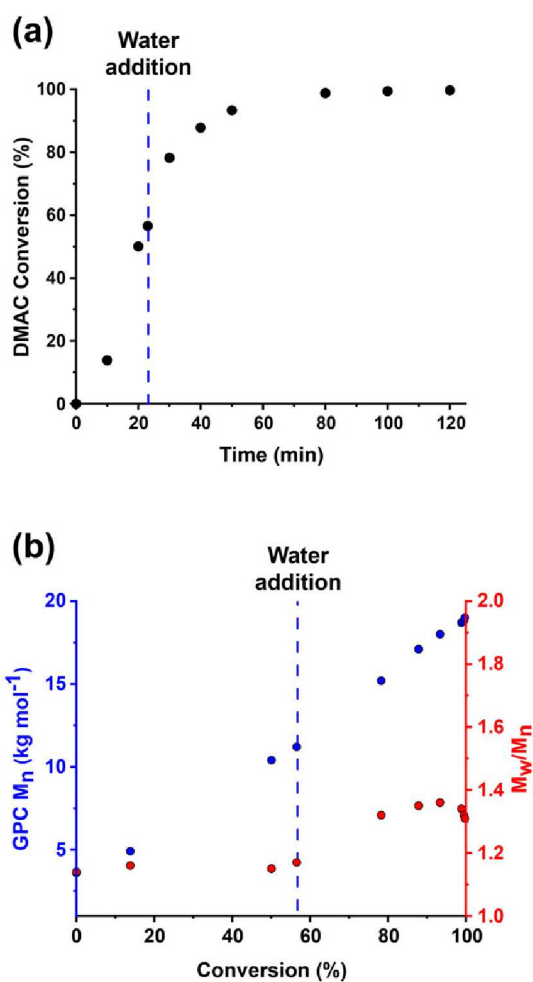


Figure 1. Kinetics of polymerization for the synthesis of PLLA₁₄-PDMAC₁₂₀ nanoparticles, where polymerization is initiated in the bulk at 70 °C followed by dilution with degassed deionized water after 23 min (DMAC conversion = 57%) to target 30% w/w solids. Conditions: [PLLA₁₄-TTC]/[ACVA] molar ratio = 10. (a) Conversion vs time curve (black data) obtained by ¹H NMR spectroscopy studies and (b) corresponding molecular weight (*M_n*, blue points) and dispersity (*M_w/M_n*, red points) vs conversion data obtained by DMF GPC analysis (expressed relative to a series of PMMA calibration standards). Selected GPC traces are shown in Figure S5.

the bulk.^{29,30} GPC analysis indicated a linear increase in molecular weight (M_n) with conversion, suggesting a well-controlled RAFT polymerization. Dispersities always remained less than 1.40 ($M_w/M_n = 1.15$ to 1.36) but were nevertheless relatively high for a RAFT polymerization (see Figure 1b). This is attributed to the chemical structure of the RAFT agent, which is not optimized for the well-controlled polymerization of DMAC.

Indeed, a control experiment conducted using the same hydroxyl-functional RAFT agent to target a PDMAC₁₀₀ homopolymer via RAFT polymerization (initially in the bulk followed by dilution with water to 30% w/w solids at an intermediate conversion of 45%) afforded more than 99% conversion after 16 h at 70 °C. GPC analysis indicated an M_n of 10.3 kg mol⁻¹ and an M_w/M_n of 1.26, which is somewhat higher than those reported in the literature for such syntheses.^{31,32} The same synthetic protocol was then used to target a series of PLLA₁₄-PDMAC_{70–300} diblock copolymers. GPC analysis indicated a linear increase in molecular weight when targeting higher PDMAC DPs with final dispersities as low as 1.28 (Table 1 and Figure 2). UV GPC ($\lambda = 305$ nm)

Table 1. Summary of Dilution Times, Intermediate DMAC Conversions, and Molecular Weight Data Obtained for a Series of PLLA₁₄-PDMAC_{70–300} Nanoparticles and PLLA₃₄-PDMAC₁₅₀ Nanoparticles^a

target diblock copolymer composition	dilution time/min	intermediate DMAC conversion %	M_n /kg mol ⁻¹	M_w/M_n
PLLA ₁₄ -TTC	N/A	N/A	3.6	1.14
PLLA ₁₄ -PDMAC ₇₀	32	58	11.5	1.40
PLLA ₁₄ -PDMAC ₉₀	60	65	13.7	1.44
PLLA ₁₄ -PDMAC ₁₁₀	40	50	16.7	1.36
PLLA ₁₄ -PDMAC ₁₃₀	30	62	17.5	1.31
PLLA ₁₄ -PDMAC ₁₅₀	35	35	19.7	1.35
PLLA ₁₄ -PDMAC ₁₇₀	28	40	23.1	1.31
PLLA ₁₄ -PDMAC ₁₉₀	32	38	24.7	1.28
PLLA ₁₄ -PDMAC ₂₁₀	21	26	28.3	1.29
PLLA ₁₄ -PDMAC ₂₃₀	26	43	29.1	1.28
PLLA ₁₄ -PDMAC ₃₀₀	29	13	40.4	1.28
PLLA ₃₄ -TTC	N/A	N/A	9.2	1.18
PLLA ₃₄ -PDMAC ₁₅₀	20	43	24.4	1.20

^aMore than 99% DMAC conversion was achieved for all diblock copolymer syntheses.

studies indicated reasonably high chain extension efficiencies when targeting PDMAC DPs up to 210, suggesting minimal contamination by the PLLA₁₄-TTC precursor (<10% residual precursor, see Figure S6).

However, when targeting a PDMAC DP of either 230 or 300, a low molecular weight species corresponding to 15–17% of the total signal was observed. Interestingly, such contamination was not discernible when using a refractive index detector, see Figure 2a. Moreover, ¹H NMR spectroscopy analysis indicated that more than 99% DMAC conversion was achieved for all syntheses, see Figure S2.

When targeting lower PDMAC DPs of either 50 or 60, problems were encountered when attempting similar syntheses at 70 °C. No precipitation was observed on dilution with water (after 45 or 37 min, respectively). However, DMF GPC analysis using a refractive index detector indicated a bimodal GPC trace in each case, suggesting poor chain extension efficiency (see Figure S7). Furthermore, no high molecular

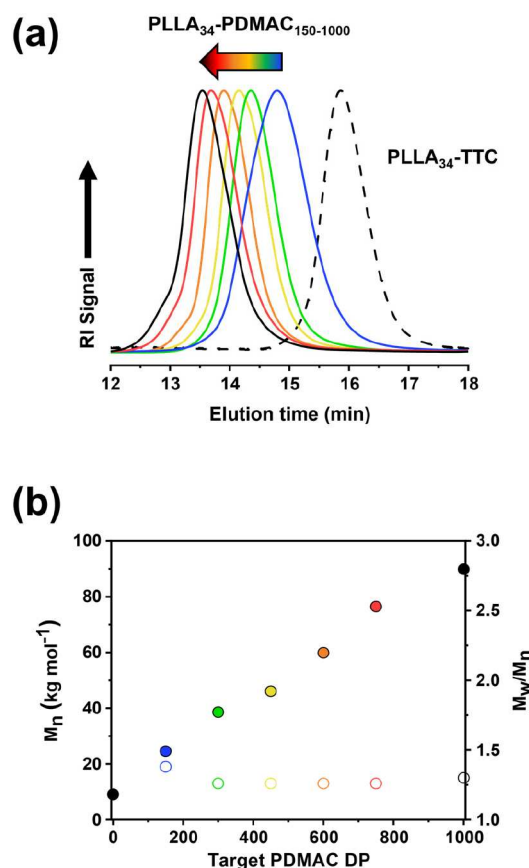


Figure 2. (a) DMF GPC curves (refractive index detector) recorded for a series of PLLA₁₄-PDMAC_{70–300} diblock copolymers and the corresponding PLLA₁₄-TTC homopolymer. Each copolymer was prepared by reverse sequence aqueous PISA at 70 °C. (b) Corresponding number-average molecular weight (M_n) and dispersity (M_w/M_n) data plotted against the target PDMAC DP.

weight species were detected by UV GPC analysis. This indicates that such DMAC polymerizations are poorly controlled because these longer chains do not possess RAFT end-groups (see Figure S7). Moreover, targeting PDMAC DPs below 50 resulted in immediate macroscopic precipitation after dilution with water. Presumably, this is simply because the PDMAC chains that are present when water is added to the reaction mixture are too short to confer effective steric stabilization on the nascent nanoparticles. In contrast, if such syntheses were conducted at 90 °C, then PDMAC DPs as low as 40 could be targeted (see Figure S8).

TEM analysis of the series of PLLA₁₄-PDMAC_{70–300} nanoparticles confirmed that the final copolymer morphology depended on the target PDMAC DP. Targeting the highest PDMAC DP of 300 led to the formation of diamond-like platelets (see Figure 3a). In contrast, short rod-like nanoparticles were obtained when targeting the lowest PDMAC DP of 70 (see Figure 3i). Hence our new approach to CDSA enables the efficient formation of highly concentrated aqueous dispersions of anisotropic nanoparticles. We believe this to be an important advance, but the diamond platelets are currently less uniform than those obtained during traditional relatively slow CDSA syntheses performed in dilute solution.^{33–35} However, certain applications such as Pickering emulsifiers and foam stabilizers do not require particularly uniform nanoparticles. In such cases, the ability to prepare anisotropic

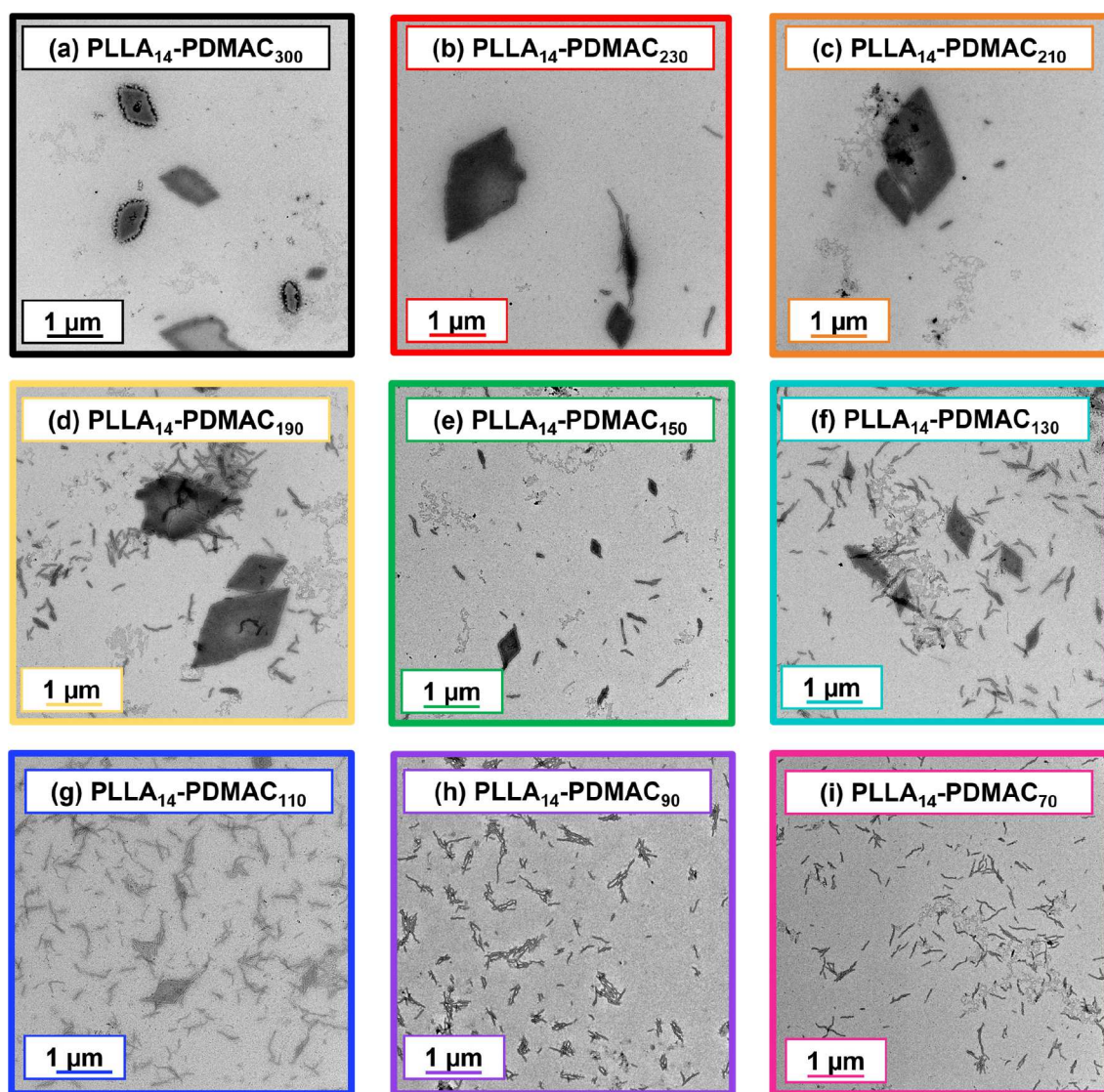


Figure 3. Representative TEM images recorded for dilute aqueous dispersions of a series of PLLA₁₄-PDPMAC_{70–300} nanoparticles: (a) $x = 300$, (b) 230, (c) 210, (d) 190, (e) 150, (f) 130, (g) 110, (h) 90, and (i) 70.

nanoparticles at high solids concentrations directly in water is likely to be a decisive advantage.

Various binary mixtures of these two morphologies were observed for intermediate PDPMAC DPs (Figure 3b–g). These observations are in good agreement with literature reports for the self-assembly of PLLA-PDPMAC diblock copolymers via CDSA in dilute solution using organic solvents such as methanol or ethanol.^{11,33} It is perhaps worth emphasizing that the design rules for PISA differ significantly from those of CDSA. Our prior reverse sequence PISA syntheses invariably yielded a spherical morphology.^{23,36} This is because such formulations always require a relatively large volume of hydrophilic monomer to solubilize the hydrophobic precursor, which inevitably leads to a relatively long steric stabilizer block. Such diblock copolymer compositions are known to favor the formation of spheres, rather than worms or vesicles.²² In contrast, when using crystalline PLLA (or PDLA), it is clear from the CDSA literature that a relatively long steric stabilizer block is essential for the formation of diamond platelets.^{33–35} Hence the judicious combination of reverse sequence PISA with CDSA is an important advance because it provides access

to a significantly wider range of copolymer morphologies. The mean % degree of crystallinity, D_c , of the PLLA₁₄-PDPMAC₃₀₀ platelets and PLLA₁₄-PDPMAC₇₀ rods was determined by X-ray diffraction (XRD), see Figure 4. The diffraction pattern recorded for the PLLA₁₄-TTC precursor has a Bragg peak at 17° that corresponds well to that reported in the literature.³⁷ The D_c for this reference sample was 41%. Similarly, D_c values of 16% and 2% were calculated for PLLA₁₄-PDPMAC₇₀ and PLLA₁₄-PDPMAC₃₀₀, respectively.

Aqueous electrophoresis studies confirmed that both PLLA₁₄-PDPMAC₃₀₀ and PLLA₁₄-PDPMAC₇₀ nanoparticles exhibited essentially zero zeta potentials from pH 4 to 9 (see Figure S9), which is consistent with the non-ionic nature of the PDPMAC steric stabilizer chains. Differential scanning calorimetry (DSC) studies were performed to examine whether the PLLA₁₄-TTC precursor exhibited crystallinity (see Figure S1). As expected, a well-defined glass transition temperature (T_g), crystallization temperature (T_c), and melting temperature (T_m) were observed.³⁸ Notably, since the T_m for PLLA₁₄-TTC is around 114 °C, this precursor should be able to direct CDSA

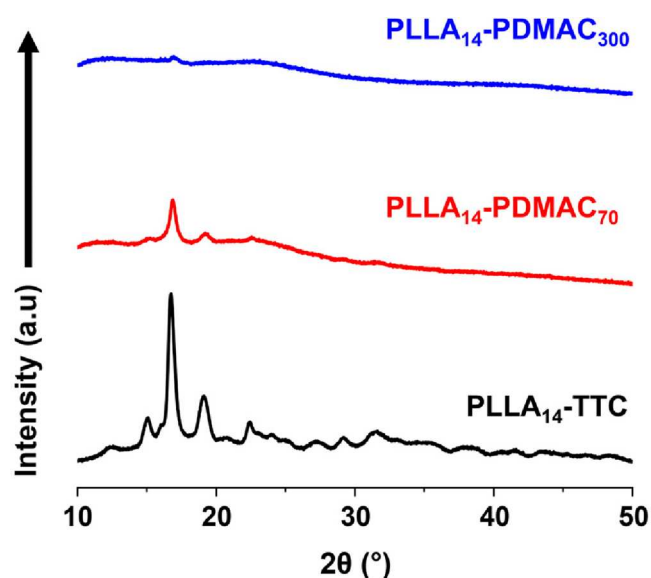


Figure 4. XRD patterns recorded for the PLLA₁₄-TTC precursor, freeze-dried PLLA₁₄-PDMAC₇₀ rod-like nanoparticles, and freeze-dried PLLA₁₄-PDMAC₃₀₀ platelets.

given that the *in situ* DMAC polymerization is conducted at 70 °C.^{1,2,4–11}

Given that (i) the DMAC polymerization is initially performed in the bulk and (ii) the DMAC monomer is a good solvent for both PLLA and PDMAC, no *in situ* self-assembly should occur prior to addition of water at a suitable intermediate DMAC conversion. Since water is a bad solvent for PLLA and a good solvent for PDMAC, its addition should result in immediate self-assembly of the growing diblock copolymer chains to form nascent PLLA-core nanoparticles. More specifically, PLLA₁₄-PDMAC₇₀ and PLLA₁₄-PDMAC₃₀₀ reaction mixtures were diluted with water after 32 and 29 min, respectively. The corresponding instantaneous DMAC conversions were 58 and 13%, which correspond to unreacted DMAC/water mass ratios of 1:3 and 1:7, respectively. These concentrated aqueous dispersions were then immediately further diluted to 0.1% w/w for TEM studies, which indicated the formation of nascent spherical aggregates in each case, see Figure 5. However, the final copolymer morphology was either

rods or platelets after annealing for 16 h (>99% DMAC conversion). In traditional CDSA syntheses, thermal annealing is important for the growth of the initial copolymer seeds to form the final anisotropic nanoparticles.^{39,40} Accordingly, we examined the effect of annealing PLLA₁₄-PDMAC_{70–300} nanoparticles at 70 °C. When targeting PLLA₁₄-PDMAC₇₀ nanoparticles, ¹H NMR studies indicated more than 99% DMAC conversion within 2 h at 70 °C. TEM analysis indicated the presence of rod-like nanoparticles at this time point, but some aggregates were also observed, see Figure 5. Annealing at 70 °C for 6 h leads to the disappearance of these aggregates, with no further change in copolymer morphology being observed up to 16 h. The corresponding DLS experiments corroborate the TEM studies: *z*-average diameters of 224 and 194 nm were obtained after 2 and 6 h, respectively. After 16 h, the *z*-average diameter remained almost unchanged at 190 nm.

Similarly, more than 99% DMAC conversion was achieved within 2 h when targeting PLLA₁₄-PDMAC₃₀₀ platelets. At this time point, diamond platelets can be observed with a mean long axis of up to 1.3 μm, see Figure 5. Annealing at 70 °C led to the formation of progressively larger diamond platelets: the mean long axis of 1.7 μm observed after 4 h increased to 1.9 μm after 6 h and 2.3 μm after 16 h. Again, DLS studies are consistent with these observations: the apparent *z*-average diameter increased from 74 nm after 2 h to 225 nm after 16 h. It is perhaps worth emphasizing that these DLS values differ significantly from the mean long axes observed by TEM because the Stokes–Einstein equation used to calculate the *z*-average diameter assumes a spherical morphology.⁴¹ Comparable results were reported by O’Reilly and co-workers when annealing PLLA₄₈-PDMAC₁₀₀₀ diamond platelets during conventional CDSA syntheses conducted in dilute ethanol at 90 °C.³³

In another experiment, rod-like nanoparticles were targeted while varying the PLLA DP. Accordingly, PLLA₃₄-TTC and PLLA₄₈-TTC precursors were prepared via anionic ROP using the same hydroxy-functional RAFT agent and characterized by NMR and GPC analysis (see Figures S10–S12). Subsequently, each precursor was chain-extended in turn with DMAC, initially via bulk polymerization followed by dilution with water at intermediate conversion.

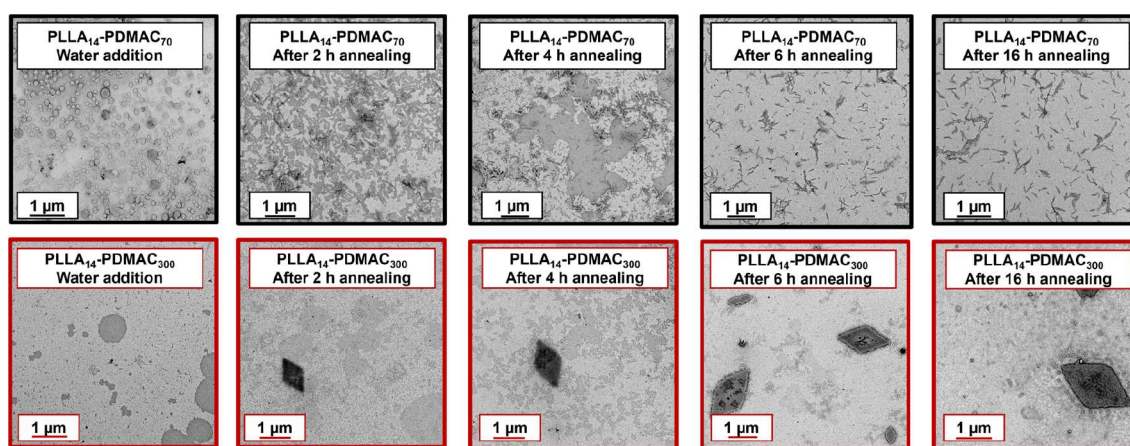


Figure 5. Representative TEM images recorded immediately after water addition for the synthesis of PLLA₁₄-PDMAC₇₀ nanoparticles (images with black outline) and PLLA₁₄-PDMAC₃₀₀ nanoparticles (images with red outline) and after annealing for 2, 4, 6, and 16 h.

Unfortunately, the PLLA₄₈-TTC precursor could not be molecularly dissolved in the DMAC monomer: the initial reaction mixture remained slightly turbid even at 70 °C. Subsequent chain extension when targeting a PDMAC DP of 400 produced an ill-defined copolymer with a dispersity above 1.80. Moreover, increasing the reaction temperature up to 90 °C did not alleviate this problem: the initial reaction mixture was always turbid rather than transparent. Thus the new approach reported herein may be limited to relatively short PLLA DPs, at least when using DMAC monomer. Nevertheless, this is sufficient to provide access to higher order morphologies.

In contrast, the PLLA₃₄-TTC precursor proved to be soluble in DMAC monomer at 70 °C when targeting a DP of 150, and the ensuing polymerization resulted in reasonably well-defined diblock copolymers ($M_w/M_n = 1.20$) at a final concentration of 30% w/w solids, see Table 1 and Figure 6. Furthermore, UV

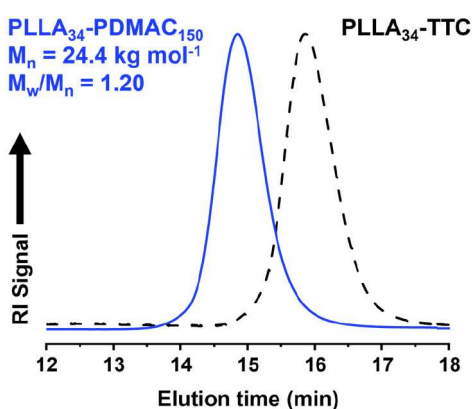


Figure 6. DMF GPC curves (refractive index detector) recorded for a PLLA₃₄-PDMAC₁₅₀ diblock copolymer (blue trace) and the corresponding PLLA₃₄-TTC homopolymer (black trace). The diblock copolymer was prepared by CDSA using a reverse sequence aqueous PISA formulation at 70 °C.

GPC analysis confirmed no significant contamination from the PLLA₃₄ precursor (see Figure S13). In this case, the final reaction mixture formed a thick paste. XRD analysis indicated D_c values of 31% and 12% for the PLLA₃₄-TTC precursor and PLLA₃₄-PDMAC₁₅₀ rod-like nanoparticles, respectively (see Figure S14). TEM analysis of dilute aqueous dispersions of the PLLA₃₄-PDMAC₁₅₀ nanoparticles confirmed that a rod-like morphology was formed when targeting a PDMAC DP of 150, see Figure S15.

The effect of varying the final nanoparticle concentration was also examined. Hence PLLA₃₄-PDMAC₁₅₀ nanoparticles were prepared at 20 and 40% w/w solids to compare with syntheses targeting 30% w/w solids. In both cases, reasonably well-defined diblock copolymer chains were obtained with dispersities of 1.26 and 1.29 respectively, see Figure S16. Furthermore, the same rod-like morphology was obtained when targeting 40% w/w solids, see Figure 7. In contrast, only ill-defined aggregates were obtained when targeting 20% w/w solids, see Figure S15.

For the same target PLLA₃₄-PDMAC₁₅₀ nanoparticles prepared at 30% w/w solids, the time at which water was added to the reaction mixture was systematically varied. No macroscopic precipitation was observed regardless of whether such dilution occurred after 10, 15 or 20 min (which corresponds to intermediate DMAC conversions of 19, 38

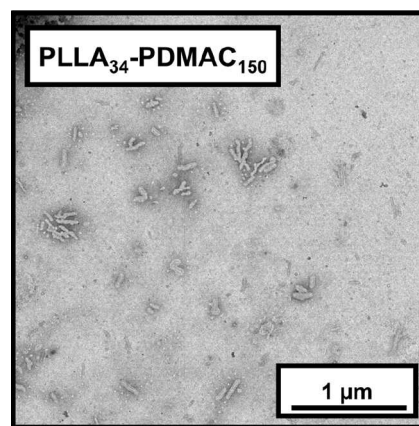


Figure 7. Representative TEM image recorded for a dilute aqueous dispersion of PLLA₃₄-PDMAC₁₅₀ nanoparticles prepared at 40% w/w solids.

and 43%, respectively). Essentially the same diblock copolymer chains were produced when water was added after either 15 or 20 min (see Figure S17) and a rod-like morphology was obtained in each case (see Figures S15b and S18). In contrast, a significantly lower copolymer molecular weight and a higher dispersity were obtained when water was added after 10 min. This suggests the loss of RAFT control under the latter conditions, presumably because the nascent PDMAC chains are too short to confer effective steric stabilization. Water addition was also attempted after 25 min. However, the reaction mixture had solidified at this time point and could not be diluted. Nevertheless, these experiments suggest that our new reverse sequence aqueous PISA plus CDSA protocol can be used to target a range of final copolymer concentrations and is reasonably tolerant of the precise time chosen for water addition.

Finally, a second hydrophilic vinyl monomer was briefly examined. Accordingly, *N*-acryloylmorpholine (NAM) was used as an alternative hydrophilic monomer to DMAC when targeting a DP of either 100 or 400 using the PLLA₁₄-TTC precursor. Essentially full NAM conversion was achieved (see Figure S19), but copolymer dispersities were broader than those achieved with the DMAC monomer (see Figure S20). More specifically, copolymer dispersities of 1.54 and 1.69 were obtained when targeting PLLA₁₄-PNAM₄₀₀ and PLLA₁₄-PNAM₁₀₀, respectively. Furthermore, when targeting a PNAM DP of 400, the chain extension efficiency was estimated to be only around 75%. Targeting a mean DP of 100 resulted in rod-like nanoparticles, see Figure 8. However, no well-defined aggregates could be obtained when targeting PLLA₁₄-PNAM₄₀₀.

PLLA is widely recognized to be hydrolytically degradable owing to the cleavable ester bonds within its backbone.⁴² Hence full degradation of this hydrophobic polyester block should yield water-soluble PDMAC chains. Accordingly, degradation studies were undertaken at 37 °C by preparing 1.0% w/w dispersions of PLLA₁₄-PDMAC₄₀ nanoparticles via dilution using an acidic, basic or neutral aqueous buffer. The rod-like morphology of the PLLA₁₄-PDMAC₄₀ nanoparticles was confirmed by TEM studies (see Figure S21). GPC was used to assess the extent of the hydrolytic degradation over time. As expected, significant degradation of the diblock copolymer chains was observed within one week for PLLA₁₄-PDMAC₄₀ nanoparticles stored at pH 10.8 (see Figure 9a).

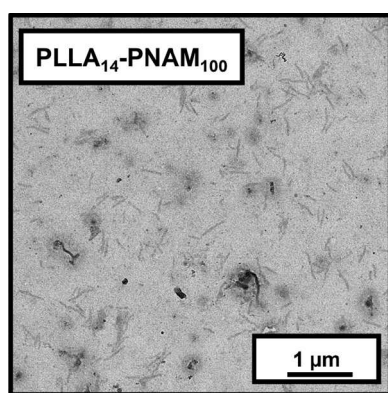


Figure 8. Representative TEM image recorded for a dilute aqueous dispersion of PLLA₁₄-PNAM₁₀₀ nanoparticles prepared at 30% w/w solids.

Hydrolytic degradation was also observed in an acidic buffer solution (pH 2.9) and in the presence of a PBS buffer (pH 7.4), albeit at a somewhat slower rate (Figure 9b,c). This is because the base-catalyzed hydrolysis of ester bonds is known to be faster than acid-catalyzed hydrolysis.⁴³ However, aging a 30% w/w aqueous dispersion of the same nanoparticles in deionized water (pH 6.7) at 20 °C led to minimal discernible degradation over four weeks (see Figure 9d). Furthermore, these PLLA₁₄-PDMAC₄₀ nanoparticles retained their colloidal stability over the same time period (see Figure S22).

DLS studies of these rod-like PLLA₁₄-PDMAC₄₀ nanoparticles in mildly basic solution (pH 10.8) confirmed a significant reduction in light scattering count rate from 56,000 to 5000 kcps within four weeks. This suggests that the original nanoparticles are converted into water-soluble PDMAC₄₀ chains. Similarly, GPC analysis confirmed that the diblock copolymer M_n was reduced from 9.6 to 5.7 kg mol⁻¹ within 24 h during an accelerated aging experiment performed at 60 °C in the presence of 5.0% w/w aqueous KOH, indicating complete degradation of the PLLA block. Concomitant DLS studies indicated a substantial reduction in the light scattering count rate from 60,000 to 500 kcps, while the number-average particle diameter was reduced from 160 to 2.8 nm. This is consistent with nanoparticle dissolution to form water-soluble PDMAC chains. One reviewer of this manuscript has pointed out that this non-degradable component comprises the majority of the mass of the original nanoparticles.

CONCLUSIONS

In summary, reverse sequence PISA has been combined with CDSA to enable the efficient preparation of 30% w/w aqueous dispersions of highly anisotropic hydrolytically degradable PLLA₁₄-PDMAC_x diblock copolymer nanoparticles. The crystalline nature of the hydrophobic PLLA block produces either diamond-like platelets (e.g., PLLA₁₄-PDMAC₃₀₀) or short rod-like particles (e.g., PLLA₁₄-PDMAC₇₀). ¹H NMR spectroscopy analysis confirms that approximately 99% DMAC conversion is achieved within 100 min at 70 °C when targeting PLLA₁₄-PDMAC₁₂₀. A linear increase in molecular weight with increasing conversion is observed, but relatively broad molecular weight distributions are observed owing to the use of a suboptimal RAFT agent. Nevertheless, M_w/M_n values do not exceed 1.44 for syntheses conducted at 70 °C, and this minor technical problem should be readily addressable in the future. Given that these anisotropic nanoparticles are prepared

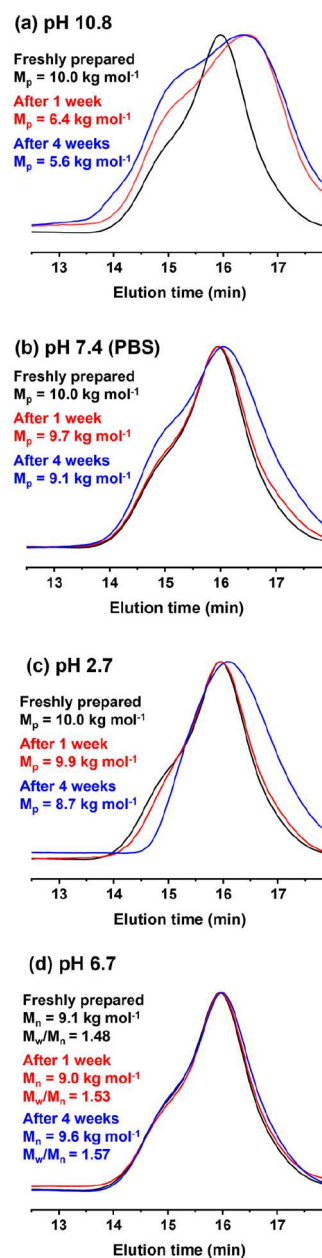


Figure 9. DMF GPC curves (refractive index detector) recorded for freshly prepared PLLA₁₄-PDMAC₄₀ and after hydrolytic degradation of 1.0% w/w aqueous dispersions of PLLA₁₄-PDMAC₄₀ nanoparticles after storage at 37 °C for either 1 or 4 weeks at (a) pH 10.8, (b) pH 7.4 (PBS buffer), (c) pH 2.7, and (d) after storage at 20 °C as a 30% w/w aqueous dispersion at pH 6.7 (red curve) for either 1 or 4 weeks.

directly in concentrated aqueous media, this is the first truly viable route for their industrial manufacture. Furthermore, preliminary data suggest that a PLLA₃₄ precursor and an alternative hydrophilic vinyl monomer (NAM) can be employed for such syntheses. Importantly, such nanoparticles are susceptible to hydrolytic degradation. We anticipate that this highly convenient new synthetic protocol should aid the evaluation of these anisotropic nanoparticles as next-generation sustainable Pickering emulsifiers³⁴ and foam stabilizers.⁴⁴

■ ASSOCIATED CONTENT

SI Supporting Information

The Supporting Information is available free of charge at <https://pubs.acs.org/doi/10.1021/jacs.4c06299>.

Full experimental details, including materials, instrumentation, analytical protocols, and synthetic protocols, summary table of reagent quantities used for polymerizations, additional NMR, DSC, and GPC data for the PLLA precursor, further GPC, NMR, TEM, DLS, and aqueous electrophoresis data for the PLLA-based diblock copolymers, and GPC and DLS hydrolytic degradation data for control experiments (PDF)

■ AUTHOR INFORMATION

Corresponding Author

Steven P. Armes – Department of Chemistry, University of Sheffield, Sheffield, South Yorkshire S3 7HF, U.K.; orcid.org/0000-0002-8289-6351; Email: s.p.arnes@sheffield.ac.uk

Authors

Matthew A. H. Farmer – Department of Chemistry, University of Sheffield, Sheffield, South Yorkshire S3 7HF, U.K.; orcid.org/0009-0008-9645-6921

Osama M. Musa – Ashland Specialty Ingredients, Bridgewater, New Jersey 08807, United States

Complete contact information is available at: <https://pubs.acs.org/doi/10.1021/jacs.4c06299>

Notes

The authors declare the following competing financial interest(s): The industrial sponsor of this study (Ashland) has recently filed a patent application to protect the associated IP.

■ ACKNOWLEDGMENTS

EPSRC is thanked for funding a CASE PhD studentship for the first author and for an Established Career Particle Technology Fellowship (EP/R003009) for the corresponding author. Ashland Specialty Ingredients (Bridgewater, New Jersey, USA) is thanked for financial support of this PhD project and for permission to publish this work. T. S. Jackson is thanked for recording the XRD spectra. This study is dedicated to the memory of Prof. Ian Manners FRS, whose seminal studies in the field of CDSA have inspired so many scientists.

■ REFERENCES

- (1) Massey, J.; Power, K. N.; Manners, I.; Winnik, M. A. Self-Assembly of a Novel Organometallic–Inorganic Block Copolymer in Solution and the Solid State: Nonintrusive Observation of Novel Wormlike Poly(ferrocenyldimethylsilane)-b-Poly(dimethylsiloxane) Micelles. *J. Am. Chem. Soc.* **1998**, *120*, 9533–9540.
- (2) Wang, X.; Guerin, G.; Wang, H.; Wang, Y.; Manners, I.; Winnik, M. A. Cylindrical Block Copolymer Micelles and Co-Micelles of Controlled Length and Architecture. *Science* **2007**, *317*, 644–647.
- (3) Teng, F.; Xiang, B.; Liu, L.; Varlas, S.; Tong, Z. Precise Control of Two-Dimensional Hexagonal Platelets via Scalable, One-Pot Assembly Pathways Using Block Copolymers with Crystalline Side Chains. *J. Am. Chem. Soc.* **2023**, *145*, 28049–28060.
- (4) Ellis, C. E.; Garcia-Hernandez, J. D.; Manners, I. Scalable and Uniform Length-Tunable Biodegradable Block Copolymer Nanofibers with a Polycarbonate Core via Living Polymerization-Induced

Crystallization-Driven Self-Assembly. *J. Am. Chem. Soc.* **2022**, *144*, 20525–20538.

(5) Li, X.; Gao, Y.; Boott, C. E.; Hayward, D. W.; Harniman, R.; Whittell, G. R.; Richardson, R. M.; Winnik, M. A.; Manners, I. Cross⁺ Supramicelles via the Hierarchical Assembly of Amphiphilic Cylindrical Triblock Comicelles. *J. Am. Chem. Soc.* **2016**, *138*, 4087–4095.

(6) Lunn, D. J.; Gould, O. E. C.; Whittell, G. R.; Armstrong, D. P.; Mineart, K. P.; Winnik, M. A.; Spontak, R. J.; Pringle, P. G.; Manners, I. Microfibres and Macroscopic Films from the Coordination-Driven Hierarchical Self-Assembly of Cylindrical Micelles. *Nat. Commun.* **2016**, *7*, 12371.

(7) Arno, M. C.; Inam, M.; Coe, Z.; Cambridge, G.; Macdougall, L. J.; Keogh, R.; Dove, A. P.; O'Reilly, R. K. Precision Epitaxy for Aqueous 1D and 2D Poly(ϵ -Caprolactone) Assemblies. *J. Am. Chem. Soc.* **2017**, *139*, 16980–16985.

(8) Petzetakis, N.; Dove, A. P.; O'Reilly, R. K. Cylindrical Micelles from the Living Crystallization-Driven Self-Assembly of Poly(Lactide)-Containing Block Copolymers. *Chem. Sci.* **2011**, *2*, 955–960.

(9) Yu, W.; Foster, J. C.; Dove, A. P.; O'Reilly, R. K. Length Control of Biodegradable Fiber-Like Micelles via Tuning Solubility: A Self-Seeding Crystallization-Driven Self-Assembly of Poly(ϵ -Caprolactone)-Containing Triblock Copolymers. *Macromolecules* **2020**, *53*, 1514–1521.

(10) Sun, L.; Petzetakis, N.; Pitto-Barry, A.; Schiller, T. L.; Kirby, N.; Keddie, D. J.; Boyd, B. J.; O'Reilly, R. K.; Dove, A. P. Tuning the Size of Cylindrical Micelles from Poly(L-Lactide)-b-Poly(Acrylic Acid) Diblock Copolymers Based on Crystallization-Driven Self-Assembly. *Macromolecules* **2013**, *46*, 9074–9082.

(11) Yu, W.; Inam, M.; Jones, J. R.; Dove, A. P.; O'Reilly, R. K. Understanding the CDSA of Poly(Lactide) Containing Triblock Copolymers. *Polym. Chem.* **2017**, *8*, 5504–5512.

(12) Nazemi, A.; Boott, C. E.; Lunn, D. J.; Gwyther, J.; Hayward, D. W.; Richardson, R. M.; Winnik, M. A.; Manners, I. Monodisperse Cylindrical Micelles and Block Comicelles of Controlled Length in Aqueous Media. *J. Am. Chem. Soc.* **2016**, *138*, 4484–4493.

(13) Finnegan, J. R.; Pilkington, E. H.; Alt, K.; Rahim, M. A.; Kent, S. J.; Davis, T. P.; Kempe, K. Stealth Nanorods via the Aqueous Living Crystallisation-Driven Self-Assembly of Poly(2-Oxazoline)S. *Chem. Sci.* **2021**, *12*, 7350–7360.

(14) Wang, Z.; Lin, M.; Bonduelle, C.; Li, R.; Shi, Z.; Zhu, C.; Lecommandoux, S.; Li, Z.; Sun, J. Thermoinduced Crystallization-Driven Self-Assembly of Bioinspired Block Copolymers in Aqueous Solution. *Biomacromolecules* **2020**, *21*, 3411–3419.

(15) Yu, Q.; Roberts, M. G.; Pearce, S.; Oliver, A. M.; Zhou, H.; Allen, C.; Manners, I.; Winnik, M. A. Rodlike Block Copolymer Micelles of Controlled Length in Water Designed for Biomedical Applications. *Macromolecules* **2019**, *52*, 5231–5244.

(16) An, Z.; Shi, Q.; Tang, W.; Tsung, C. K.; Hawker, C. J.; Stucky, G. D. Facile RAFT Precipitation Polymerization for the Microwave-Assisted Synthesis of Well-Defined, Double Hydrophilic Block Copolymers and Nanostructured Hydrogels. *J. Am. Chem. Soc.* **2007**, *129*, 14493–14499.

(17) Charleux, B.; Delaitre, G.; Rieger, J.; D'Agosto, F. Polymerization-Induced Self-Assembly: From Soluble Macromolecules to Block Copolymer Nano-Objects in One Step. *Macromolecules* **2012**, *45*, 6753–6765.

(18) Warren, N. J.; Armes, S. P. Polymerization-Induced Self-Assembly of Block Copolymer Nano-Objects via RAFT Aqueous Dispersion Polymerization. *J. Am. Chem. Soc.* **2014**, *136*, 10174–10185.

(19) Canning, S. L.; Smith, G. N.; Armes, S. P. A Critical Appraisal of RAFT-Mediated Polymerization-Induced Self-Assembly. *Macromolecules* **2016**, *49*, 1985–2001.

(20) Penfold, N. J. W.; Yeow, J.; Boyer, C.; Armes, S. P. Emerging Trends in Polymerization-Induced Self-Assembly. *ACS Macro Lett.* **2019**, *8*, 1029–1054.

- (21) Wang, X.; An, Z. New Insights into RAFT Dispersion Polymerization-Induced Self-Assembly: From Monomer Library, Morphological Control, and Stability to Driving Forces. *Macromol. Rapid Commun.* **2019**, *40*, 1800325.
- (22) Blanz, A.; Ryan, A. J.; Armes, S. P. Predictive Phase Diagrams for RAFT Aqueous Dispersion Polymerization: Effect of Block Copolymer Composition, Molecular Weight, and Copolymer Concentration. *Macromolecules* **2012**, *45*, 5099–5107.
- (23) Farmer, M. A. H.; Musa, O. M.; Armes, S. P. Efficient Synthesis of Hydrolytically Degradable Block Copolymer Nanoparticles via Reverse Sequence Polymerization-Induced Self-Assembly in Aqueous Media. *Angew. Chem.* **2023**, *62*, No. e202309526.
- (24) Similar findings were recently reported by a French team; see Grazon, C.; Salas-Ambrosio, P.; Ibarboure, E.; Buol, A.; Garanger, E.; Grinstaff, M. W.; Lecommandoux, S.; Bonduelle, C. Aqueous Ring-Opening Polymerization-Induced Self-Assembly (ROPISA) of N-Carboxyanhydrides. *Angew. Chem. Int. Ed.* **2020**, *59*, 622–626. In this prior study, ring-opening polymerization of N-carboxyanhydrides was performed using a poly(ethylene glycol) macroinitiator. This formulation produced anisotropic rods at 13% w/w solids with an overall yield of 77–87%. In the present study, either short rods or diamond platelets can be prepared in more than 99% yield at 30% w/w solids.
- (25) Samarajeewa, S.; Shrestha, R.; Li, Y.; Wooley, K. L. Degradability of Poly(Lactic Acid)-Containing Nanoparticles: Enzymatic Access through a Cross-Linked Shell Barrier. *J. Am. Chem. Soc.* **2012**, *134*, 1235–1242.
- (26) Fu, C.; Xu, J.; Kokotovic, M.; Boyer, C. One-Pot Synthesis of Block Copolymers by Orthogonal Ring-Opening Polymerization and PET-RAFT Polymerization at Ambient Temperature. *ACS Macro Lett.* **2016**, *5*, 444–449.
- (27) Chiefari, J.; Chong, Y. K. B.; Ercole, F.; Krstina, J.; Jeffery, J.; Le, T. P. T.; Mayadunne, R. T. A.; Meijs, G. F.; Moad, C. L.; Moad, G.; Rizzardo, E.; Thang, S. H. Living Free-Radical Polymerization by Reversible Addition - Fragmentation Chain Transfer: The RAFT Process. *Macromolecules* **1998**, *31*, 5559–5562.
- (28) Perrier, S. 50th Anniversary Perspective: RAFT Polymerization—A User Guide. *Macromolecules* **2017**, *50*, 7433–7447.
- (29) Schrooten, J.; Lacík, I.; Stach, M.; Hesse, P.; Büback, M. Propagation Kinetics of the Radical Polymerization of Methylated Acrylamides in Aqueous Solution. *Macromol. Chem. Phys.* **2013**, *214*, 2283–2294.
- (30) Lacík, I.; Chovancová, A.; Uhelská, L.; Preusser, C.; Hutchinson, R. A.; Büback, M. PLP-SEC Studies into the Propagation Rate Coefficient of Acrylamide Radical Polymerization in Aqueous Solution. *Macromolecules* **2016**, *49*, 3244–3253.
- (31) Zaquen, N.; Zu, H.; Kadir, A. M. N. B. P. H. A.; Junkers, T.; Zetterlund, P. B.; Boyer, C. Scalable Aqueous Reversible Addition-Fragmentation Chain Transfer Photopolymerization-Induced Self-Assembly of Acrylamides for Direct Synthesis of Polymer Nanoparticles for Potential Drug Delivery Applications. *ACS Appl. Polym. Mater.* **2019**, *1*, 1251–1256.
- (32) Moad, G.; Rizzardo, E.; Thang, S. H. Radical Addition-Fragmentation Chemistry in Polymer Synthesis. *Polymer* **2008**, *49*, 1079–1131.
- (33) Inam, M.; Cambridge, G.; Pitto-Barry, A.; Laker, Z. P. L.; Wilson, N. R.; Mathers, R. T.; Dove, A. P.; O'Reilly, R. K. 1D: Vs. 2D Shape Selectivity in the Crystallization-Driven Self-Assembly of Polylactide Block Copolymers. *Chem. Sci.* **2017**, *8*, 4223–4230.
- (34) Inam, M.; Jones, J. R.; Pérez-Madrugal, M. M.; Arno, M. C.; Dove, A. P.; O'Reilly, R. K. Controlling the Size of Two-Dimensional Polymer Platelets for Water-in-Water Emulsifiers. *ACS Cent. Sci.* **2018**, *4*, 63–70.
- (35) Zheng, J. X.; Xiong, H.; Chen, W. Y.; Lee, K.; Van Horn, R. M.; Quirk, R. P.; Lotz, B.; Thomas, E. L.; Shi, A. C.; Cheng, S. Z. D. Onsets of Tethered Chain Overcrowding and Highly Stretched Brush Regime via Crystalline - Amorphous Diblock Copolymers. *Macromolecules* **2006**, *39*, 641–650.
- (36) Farmer, M. A. H.; Musa, O. M.; Haug, I.; Naumann, S.; Armes, S. P. Synthesis of Poly(Propylene Oxide)-Poly(N,N-Dimethylacrylamide) Diblock Copolymer Nanoparticles via Reverse Sequence Polymerization-Induced Self-Assembly in Aqueous Solution. *Macromolecules* **2024**, *57*, 317–327.
- (37) Ma, B.; Wang, X.; He, Y.; Dong, Z.; Zhang, X.; Chen, X.; Liu, T. Effect of Poly(Lactic Acid) Crystallization on Its Mechanical and Heat Resistance Performances. *Polymer* **2021**, *212*, No. 123280.
- (38) Pan, P.; Kai, W.; Zhu, B.; Dong, T.; Inoue, Y. Polymorphous Crystallization and Multiple Melting Behavior of Poly(L-Lactide): Molecular Weight Dependence. *Macromolecules* **2007**, *40*, 6898–6905.
- (39) Song, S.; Yu, Q.; Zhou, H.; Hicks, G.; Zhu, H.; Rastogi, C. K.; Manners, I.; Winnik, M. A. Solvent Effects Leading to a Variety of Different 2D Structures in the Self-Assembly of a Crystalline-Coil Block Copolymer with an Amphiphilic Corona-Forming Block. *Chem. Sci.* **2020**, *11* (18), 4631–4643.
- (40) Guerin, G.; Rupa, P.; Molev, G.; Manners, I.; Jinnai, H.; Winnik, M. A. Lateral Growth of 1D Core-Crystalline Micelles upon Annealing in Solution. *Macromolecules* **2016**, *49* (18), 7004–7014.
- (41) Miller, C. C. The Stokes-Einstein Law. *Proc. R. Soc. London A* **1924**, *106*, 724–749.
- (42) Drumright, R. E.; Gruber, P. R.; Henton, D. E. Polylactic Acid Technology. *Adv. Mater.* **2000**, *12*, 1841–1846.
- (43) Parekh, V. J.; Rathod, V. K.; Pandit, A. B. Substrate Hydrolysis: Methods, Mechanism, and Industrial Applications of Substrate Hydrolysis. In *Comprehensive Biotechnology*, 2nd ed.; Academic Press, 2011; pp 103–118.
- (44) Yang, P.; Mykhaylyk, O. O.; Jones, E. R.; Armes, S. P. RAFT Dispersion Alternating Copolymerization of Styrene with N-Phenylmaleimide: Morphology Control and Application as an Aqueous Foam Stabilizer. *Macromolecules* **2016**, *49*, 6731–6742.